American Mineralogist, Volume 78, pages 565–573, 1993

Nonstoichiometry of magnetite-ulvöspinel solid solutions quenched from 1300 °C

E. Senderov, A. U. Dogan, A. Navrotsky

Department of Geological and Geophysical Sciences and Princeton Materials Institute, Princeton University, Princeton, New Jersey 08544, U.S.A.

Abstract

Magnetite-ulvöspinel (Fe_3O_4-Fe_2TiO_4) solutions were synthesized in CO_2 + H_2 atmospheres and quenched from 1300 °C to liquid N_2. The f_{O_2} during synthesis was monitored by a solid electrolyte cell (ZrO_2 with 9% Y_2O_3). There are noticeable differences in unit-cell parameters, a_0, of samples synthesized with the same Ti/Fe ratio but under different f_{O_2} conditions. The samples obtained under relatively reducing conditions at the boundary with fields containing wüstite or metallic Fe have systematically higher a_0 values than ulvöspinel coexisting with rhombohedral solid solutions or synthesized near this boundary under relatively oxidizing conditions. The change in a_0 across the solid-solution field at a fixed Ti/Fe ratio becomes more pronounced and approaches 0.01 Å for high Ti compositions. The unit-cell parameter variation at a constant Ti/Fe ratio is related to the deviation from stoichiometry [(Fe + Ti)/O < ¾] of the solution $Fe_{3-x}Ti_xO_{4+y}$. Trends were obtained in the cation to O ratio with increasing f_{O_2} at fixed Ti/Fe by direct O analysis using the electron microprobe. A gain of approximately 2 mol% O ($y = 0.08$) for quenched samples with $x \geq 0.7$ under the most oxidizing conditions is seen relative to samples quenched under reducing conditions and assumed to be stoichiometric ($y = 0$). A phase diagram in $x - f_{O_2}$ space at 1300 °C is presented.

Introduction

The study of magnetite-ulvöspinel (Fe_3O_4-Fe_2TiO_4) solutions is stimulated by their interest to the materials science community (Fe metallurgy, ferrites) and Earth science community (indicators of magnetic, redox, and thermal history of rocks). Important features of these solid solutions, though complete in terms of continuous Fe-Ti variation, are not really pseudobinary because they depart from stoichiometry, (Fe + Ti)/O < ¾, because of oxidation (Webster and Bright, 1961; Taylor, 1964; Katsura et al., 1976; Simons and Woermann, 1978).

When synthesized at low f_{O_2} in equilibrium with wüstite, magnetite-ulvöspinel solutions contain little cation excess (Dieckmann, 1982; Aragon and McCallister, 1982), and their composition varies essentially along the stoichiometric magnetite-ulvöspinel join, $Fe_{3-x}Ti_xO_4$.

As oxidation proceeds with increasing f_{O_2}, the reactions at constant cation composition produce phases enriched in O relative to cations, Ti + Fe. Keeping the total number of cations equal to 3, the magnetite-ulvöspinel solution composition could be expressed by the formula $Fe_{3-x}Ti_xO_{4+y}$, with y a convenient indicator of nonstoichiometry. However, oxidation occurs with an increase in the Fe^{3+}/Fe^{2+} ratio and with the formation of cation vacancies while the O sublattice remains intact (Dieckmann, 1982; Aragon and McCallister, 1982).

Deviations from stoichiometric compositions although noticeable, are generally small at high temperatures. Estimations of this rather narrow nonstoichiometric range are scarce and fragmentary. Taylor (1964), from gravimetric experiments at 1300 °C, suggested that the maximum amount of vacancies did not depend on the Ti content and could probably approach about 2 mol%. Similar values were obtained for magnetite from in situ high-temperature measurements (Dieckmann, 1982) and for a sample, $Fe_{2.4}Ti_{0.6}O_{4.06}$, weighed after quenching from 1275 °C (Hauptman, 1974).

Magnetite-ulvöspinel solutions can be oxidized to Ti-bearing maghemite (γ-phase) spinel at low temperatures (<400 °C). Its range of nonstoichiometry is much greater than that seen at high temperatures and includes the fully oxidized composition with no Fe^{2+} present. In the Ti-free end-member that is γ-Fe_2O_3, $Fe^{3+}_{8/3}\square_{1/3}O_4$. However, this oxidized Ti-bearing maghemite is generally poorly crystalline and metastable. The degree of oxidation and the compositional variation in these samples correlate with the observed unit-cell parameter change (Readman and O'Reilly, 1972; Nishitani and Kono, 1983; Goss, 1988).

The aim of this study was to refine the limits of compositional variation in magnetite-ulvöspinel solutions, synthesized and quenched from 1300 °C, and to determine the variation of O content with f_{O_2} and with the Fe/Ti ratio. These samples will then be used for further structural and thermochemical studies. In this paper we report the synthesis procedures, unit-cell measurements, a phase diagram in $x - f_{O_2}$ space, and compositions, both Ti/Fe ratios and O contents, based on electron microprobe analyses.

0003–004X/93/0506–0565$02.00

Experimental Methods

Starting materials and synthesis procedure

Dried Fe_2O_3 and TiO_2 (both 99.999% purity, Johnson Mathey Inc.) were used for mixture preparation. The reagents were ground together in an agate mortar under methanol, dried, pressed into pellets of 120–150 mg, and sintered in air at 1200 °C. The sintered pellets were wrapped in 0.1-mm Pt wire, suspended at the level of the hot spot in a Deltech vertical tube furnace, and annealed for 1–2 d at 1300 °C. This period significantly exceeds the estimates of time needed by 3–6 h, for Fe-Ti oxide equilibration with gas atmospheres at 1300 °C, based on weight loss and gain (Taylor, 1964; Hauptman, 1974). Microprobe analysis (see below) showed the samples to be homogeneous in Fe/Ti ratio and O content (except for oxidized quench rims, discussed below). Thus we considered it unnecessary to do several cycles of grinding and annealing. The reproducibility of temperature between experiments was ±5 °C.

A H_2-CO_2 gas mixture at total pressure of 1 atm was used to create various f_{O_2} values (Deines et al., 1974). A CO_2-O_2 atmosphere was also used to maintain higher f_{O_2} values ($\log f_{O_2} > -3$). Gas flowed from the top to the bottom of the furnace tube.

The f_{O_2} was monitored using a solid electrolyte cell of ZrO_2 with 9 wt% Y_2O_3. Total gas flow was 100 cc/min. Values of $\log f_{O_2}$ were calculated from emf measurements, with air as a reference. More details of gas flow regulation and emf measurement are in Brown et al. (in preparation). The cell was calibrated at 1300 °C against the Ni + NiO and wüstite + magnetite buffers. Equilibrium $\log f_{O_2}$ values of these reactions at 1300 °C, estimated from equations summarized by Chou (1987) vary in a range of about 0.1 in $\log f_{O_2}$ for both buffers. Our measurements fall into the cited ranges. The uncertainty in calculated $\log f_{O_2}$ values is ±0.05.

At the end of an experiment, a special bottom plug on the furnace tube was opened, the Pt wire which held the pellet was burned and the pellet fell into liquid N_2.

A potential problem is Fe loss to any Pt container or wire holding the samples. Our Pt wires were not presaturated with Fe (that would have made them too brittle to bend). However, the length of the wire, 0.1 mm in diameter, in contact with a pellet of 120–150 mg, was <30 mm, and its weight <5 mg. Even if the Pt absorbed its own weight in Fe (a worst case), the change in Fe/(Ti + Fe) in a typical sample would be on the order of 2 mol%. The microprobe analyses (see below) indeed confirmed that the analyzed ratios were within 2% or better of the stoichiometries, and the analyzed compositions were used in further calculations. Thus we believe that Fe loss is not a serious complication in these experiments.

X-ray diffraction

Quenched samples were studied by X-ray diffraction at room temperature with a Scintag PAD V powder automated diffractometer equipped with a solid-state detector. Cu$K\alpha$ radiation was used. Si (NBS reference material 640d) was used as an internal standard to correct peak positions after background and $K\alpha_2$ lines subtraction. Samples were scanned one or several times at the rate of 1 or 0.5°/min.

The lattice parameter was refined using the least-squares procedure of Appleman and Evans (1973). Some 8–15 reflections ($25° < 2\theta < 100°$) were used in each refinement.

The 2 sd error of the a_0 value refined for one X-ray pattern usually exceeds the deviation from the mean of the a_0 value for several patterns of the same sample. We show the standard deviation of the mean value, or 2 sd of the individual fit if a sample was scanned only once. In most cases the error is better than ±0.002 Å.

Electron microprobe analysis

Part of each quenched sample was polished and used for optical microscopy and electron microprobe analysis. Reflected light microscopy was used for preliminary characterization of samples to determine phase homogeneity, distribution of pores, and other features.

The Jeol JXA-8600 Superprobe at Rutgers University was used with 15-KeV accelerating voltage, and 20-nA specimen current. The beam diameter was about 1 μm. The crystals used were PET for Ti, LiF for Fe, and LDE1 for O.

Special care was taken during sample preparation. Polishing and coating of specimens in each group analyzed were performed simultaneously under the same conditions and calibrated against the same reference sample. To improve counting statistics, the counting time was increased to 100 s, which gave a standard deviation of 0.3% for O. A further increase in analysis time was not desirable because of deterioration in the O count rate due to sample damage under the electron beam. Another factor limiting count time was contamination by a precipitate, probably formed from traces of hydrocarbons polymerized by the beam.

Natural pure magnetite and ilmenite (Anderson, 1968) were used for calibration of Fe, Ti, and O. Fe was calibrated against magnetite and Ti against ilmenite. When analyzing spinel solid solution with $x < 0.5$, $\mathrm{Ti/(Ti + Fe)} < 0.166$, O was calibrated against magnetite. If $\mathrm{Ti/(Ti + Fe)} \geq 0.166$, the O was calibrated against ilmenite.

Shorter counting times (up to 1% sd) were used when routine analyses were aimed only at Ti/Fe ratio calculations.

Despite the care taken, we were not satisfied with the absolute values of O contents. Totals (Fe + Ti + O) ranged from 99 to 101%. The O contents determined depended too much on which standard (magnetite or ilmenite) was used. These problems were not surprising and are caused by the high absorption of O X-rays by other elements (which render standard correction procedures inadequate), by the lack of well-analyzed O standards, and by the high degree of accuracy and precision needed to determine small degrees of nonstoichiometry.

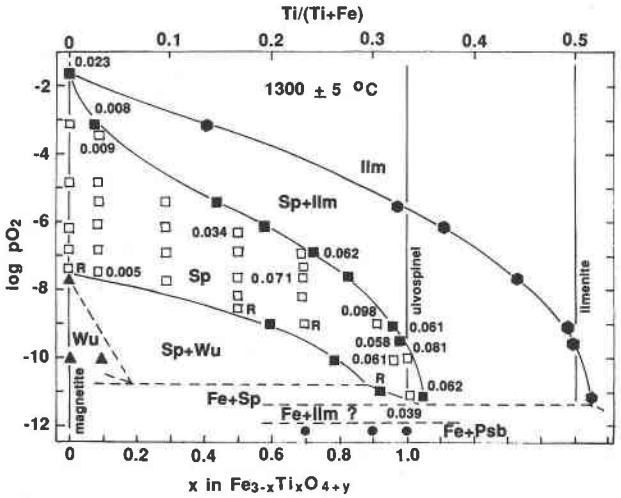

Fig. 1. Experimental data for phase diagram in Fe-Ti-O at 1300 ± 5 °C. Abbreviations: Ilm = rhombohedral hematite-ilmenite solid solutions; Sp = spinel $Fe_{3-x}Ti_xO_{4+y}$ solid solutions; Wu = $Fe_{1-x}O$ wüstite phase; Psb = pseudobrookite phase; Fe = metallic Fe phase. Phase assemblages: solid hexagons and upper solid squares = Ilm and Sp, respectively, from the Ilm + Sp assemblage; open squares = Sp, synthesized as single phase (numbers represent values of y from microprobe analyses, R = reference samples); lower solid squares = Sp from Sp + Wu; solid circles = Fe + Psb; solid triangles = Wu. Vertical lines represent Ti/(Ti + Fe) of magnetite, ulvöspinel, and ilmenite end-members.

Realizing that we needed highly precise measurements of the change in the O content with f_{O_2}, we decided to adopt a relative procedure, which provided trends in O content for samples with similar Ti/Fe ratios by using, as a standard for each group, a sample produced under low f_{O_2}, which can be assumed to be stoichiometric [(Fe + Ti)/O = ¾]. This procedure is described further below. With this procedure, the relative error in O to cation ratio determination did not exceed 1%. The error in Ti/(Ti + Fe) ratio determination was several thousandths, and the absolute error in x (mole fraction of ulvöspinel) did not exceed ±0.01. This study represents the determination of much smaller deviations from stoichiometry than the microprobe analyses of Furuta et al. (1985) on more oxidized low-temperature samples.

Results

Phase boundaries

The results of synthesis are shown in Table 1 and Figure 1. Magnetite-ulvöspinel solutions synthesized as single phases with a constant Ti/(Ti + Fe) ratio lie along vertical lines crossing the field in Figure 1. Only a gain or loss of O can be involved in change of composition along these O reaction lines. The f_{O_2} range for constant Ti/Fe composition is terminated from above by the boundary with the two-phase field of spinel + rhombohedral phase (hematite-ilmenite) and from below by spinel + wüstite or metallic Fe associations. The log f_{O_2}

Table 1. Phase equilibrium experiments, cation ratios [Ti/(Ti + Fe)], and spinel lattice parameters

Sample	t (h)	Log f_{O_2}	Phases	Ti/(Ti + Fe) (atom ratio)	a_0 of spinel (Å)
			x^* = 0		
53	22	−10.00	wüstite	0	—
71	45	−7.64	wüstite + spinel	0	—
				0	8.3960(12)
78	31	−7.43	spinel	0	8.3956(10)
30	24	−6.85	spinel	0	8.3948(10)
37	25	−6.19	spinel	0	8.3958(6)
38	24	−4.78	spinel	0	8.3960(6)
39	43	−3.12	spinel	0	8.3956(10)
87	46	−1.59	spinel +	0	8.3922(10)
			rhom. phase	0	—
			x = 0.1		
46	50	−10.02	wüstite	—	—
34	24	−7.56	spinel	0.030(1)	8.4046(12)
27	26	−6.84	spinel	0.031(3)	8.4052(16)
25	22	−6.15	spinel	0.031(2)	8.4062(6)
24	28	−5.46	spinel	0.030(1)	8.4056(10)
26	44	−4.77	spinel	0.030(1)	8.4010(9)
62	44	−3.40	spinel	0.030(1)	8.4020(8)
23	60	−3.08	spinel +	0.022(1)	8.3988(4)
			rhom. phase	0.135(2)	—
			x = 0.3		
19	32	−7.57	spinel	0.100(1)	8.4291(10)
17	22	−6.88	spinel	0.102(1)	8.4283(26)
21	48	−6.19	spinel	0.099(2)	8.4306(16)
15	50	−5.40	spinel	0.100(2)	8.4252(11)
			x = 0.5		
33	24	−9.03	spinel + wüstite	0.198(3)	8.4813(11)
				—	—
74	30	−8.54	spinel	0.167(3)	8.4660(6)
13	24	−8.20	spinel	0.169(2)	8.4637(22)
12	22	−7.57	spinel	0.167(2)	8.4645(8)
11	23	−6.87	spinel	0.169(2)	8.4612(12)
10	28	−6.15	spinel	0.164(1)	8.4610(7)
9	21	−5.42	spinel +	0.145(2)	8.4469(5)
			rhom. phase	0.324(2)	—
			x = 0.7		
6	20	−12.16	metallic Fe +	—	—
			pseudobrookite	—	—
36	36	−10.07	spinel + wüstite	0.262(4)	8.5128(4)
			(decomposed)	—	—
32	23	−9.03	spinel	0.233(1)	8.5019(10)
31	24	−8.20	spinel	0.237(3)	8.4993(14)
35	30	−7.57	spinel	0.237(3)	8.4965(7)
28	50	−7.25	spinel	0.234(1)	8.4920(6)
29	21	−6.93	spinel	0.231(1)	8.4911(14)
5	27	−6.13	spinel +	0.195(2)	8.4703(10)
			rhom. phase	0.371(2)	—
			x = 0.9		
45	20	−12.09	metallic Fe +	—	—
			pseudobrookite	—	—
51	18	−11.03	spinel +	0.311(2)	8.5336(4)
			metallic Fe	—	—
42	87	−10.06	spinel	0.322(1)	8.5298(4)
43	29	−9.04	spinel	0.304(1)	8.5241(3)
44	23	−7.59	spinel +	0.276(1)	8.5070(3)
			rhom. phase	0.443(2)	—
47	69	−6.87	spinel +	0.240(1)	8.4907(7)
			rhom. phase	0.406(3)	—
			x = 1.0		
76	23	−12.14	metallic Fe +	—	—
			pseudobrookite	—	—
72	22	−11.17	spinel	0.341(2)	8.5346(5)
54	40	−10.00	spinel	0.338(1)	8.5306(18)
75	24	−9.49	spinel +	0.328(1)	8.5266(9)
			rhom. phase	0.498(1)	—
73	40	−9.07	spinel +	0.321(1)	8.5233(12)
			rhom. phase	0.493(1)	—
			3Ti/(Ti + Fe) in starting mixture = 1.2		
83	26	−11.00	spinel +	0.355(2)	8.5340(13)
			ilmenite	0.518(1)	—

* The symbol x = 3Ti/(Ti + Fe) in starting mixture.

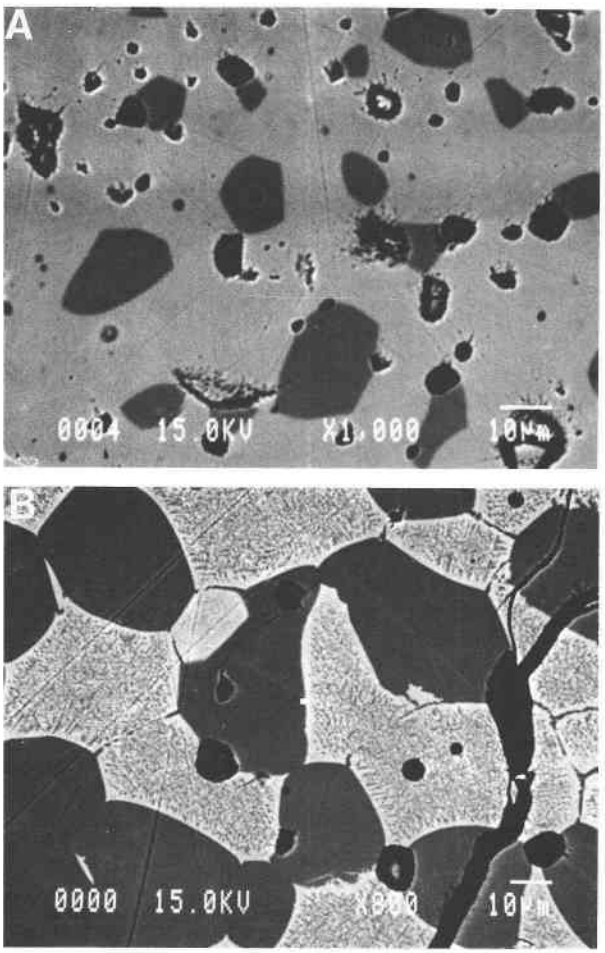

Fig. 2. Backscattered electron image of products from (**A**) magnetite-ulvöspinel solution (light) + rhombohedral phase region, sample 23, and (**B**) wüstite (light) with inclusions of Ti-containing phase + spinel region, sample 33.

values of these boundaries coincide well with Taylor's (1964) experimental data. Discrepancies are significant only under strongly reducing conditions ($\log f_{O_2} \leq -10$).

Backscattered electron images of these two-phase products are given on Figure 2. There are indications of quench phenomena. Wüstite from the two-phase region (Fig. 2B) bears evidence of high-temperature decomposition. Energy-dispersive analysis shows that a Ti-containing phase exsolved from the wüstite matrix. Some TiO_2 enters into the quenched wüstite (sample 46), but the high-temperature phase should contain a higher Ti content, at least 8.5 mol% at 1300 °C (Simons and Woermann, 1978).

The quenching phenomena appear to manifest themselves also in the formation of rims of a phase richer in O. Rims were usually observed in the two-phase products: a rhombohedral phase rim around rhombohedral phase + spinel; a spinel rim around spinel + wüstite.

A rim of magnetite formed during quenching was seen around wüstite (sample 71, Table 1). This experiment and the experiment wherein magnetite was synthesized as a single phase (sample 78) bracketed the wüstite + magnetite equilibrium, located at $\log f_{O_2} = -7.50$. The magnetite-hematite boundary is located at $\log f_{O_2} = -1.59$ by this two-phase synthesis product (sample 87). Both these equilibria confirm earlier evaluations of these buffer reaction parameters (Chou, 1987).

At low f_{O_2} (Fig. 1) an invariant equilibrium, spinel + wüstite + metallic Fe, separates the wüstite + spinel from the Fe + spinel regions. The f_{O_2} values of this equilibrium must be between $\log f_{O_2} = -10.07$ (spinel + wüstite, sample 36) and $\log f_{O_2} = -11.03$ (spinel + metallic Fe, sample 51). This is in agreement with the estimation of the invariant equilibrium at $\log f_{O_2} = -10.65$ (Simons and Woermann, 1978). The equilibrium marks a break on the lower boundary of the spinel field because the boundary curve must change slope when transferring from the association of wüstite + spinel to the Fe + spinel. Spinel equilibrated with wüstite is assumed to have virtually stoichiometric O content. The change of slope then means a departure from magnetite-ulvöspinel stoichiometry. The limiting point of stoichiometric phase stability is at approximately 90 mol% ulvöspinel. Spinels with $x > 0.9$ can have only nonstoichiometric compositions.

High-Ti specimens can have a noticeable excess of Ti over the ideal ratio in ulvöspinel of Ti/(Fe + Ti) = 0.333, for example, spinel no. 83, Tables 1, 2. This spinel, with Ti/(Fe + Ti) = 0.355 was produced at $\log f_{O_2} = -11.00$ with ilmenite, which was nonstoichiometric too, under conditions approaching those of invariant equilibrium spinel + ilmenite + Fe, which defines the lowest f_{O_2} of the ulvöspinel stability range.

Under strongly reducing conditions, Fe becomes significantly volatile. Ti-rich spinels formed under these conditions have a Ti/Fe ratio that differs from that of the starting material because of Fe loss, especially after longer experiments (sample 42 in Table 1). This is also the region where the Fe loss to Pt is greatest.

Unit-cell parameters

Variation in the unit-cell parameter, a_0, along the O-reaction lines may indicate stoichiometric change at a constant Ti/(Ti + Fe) ratio (see Fig. 3). The unit-cell parameter decreases as f_{O_2} increases. When $x \geq 0.7$, the range of a_0 variation becomes as great as approximately 0.01 Å.

In the Fe-rich part of the system, the changes in a_0 are not so pronounced, despite the wider range of f_{O_2} variation. A decrease of a_0 near the high f_{O_2} boundary can be detected, however, even for magnetite-rich compositions.

Electron microprobe analysis

To avoid problems of incompatibility of O determinations when samples had different Ti/Fe ratios, we divided analyses into groups with narrow ranges in composition (Table 2, Fig. 1).

Within each group, we chose a reference sample that was essentially stoichiometric with respect to O. These were samples 78, 74, and 32, which were synthesized at

conditions near the stability of wüstite + spinel, and sample 51, which was equilibrated at conditions near the wüstite + Fe + spinel invariant equilibrium (Fig. 1). The assumption that these samples are essentially stoichiometric (three cations to four O atoms) relies on the work of Dieckmann (1982) for magnetite and Simons and Woermann (1978) for magnetite-ulvöspinel solutions. Instead of cation vacancies and a full O sublattice [corresponding to (Fe + Ti)/O < ¾], under strongly reducing conditions there is a slight metal excess (O deficiency), accommodated by cation interstitials, and resulting in (Fe + Ti)/O > ¾. However, the extent of this O loss is at least an order of magnitude less than that of the O gain under oxidizing conditions, and, thus, from the point of view of the analysis here, these samples can be assumed stoichiometric in metal to O ratio (though some Ti^{3+} may be present).

Averaged values for several analyses of each sample are given in Table 2. Standard deviation for each set is given in parentheses. The amounts of Fe, Ti, and O were used to calculate cation to cation and O to cation ratios. To eliminate probable systematic uncertainties in O results, the O to cation ratios were corrected on the basis of the assumption that, in the reference sample, this ratio must be O/(Ti + Fe) = ⅓.

Taking into account that the systematic error for all samples within the same group is the same, we found a group correction factor, C, common to each group. For the assumed stoichiometric reference sample, with r = O/(Ti + Fe),

$$C = r(\text{stoich})/r(\text{obs}) = 1.333/r(\text{obs}). \quad (1)$$

For other analyzed samples in the same group [with similar Ti/(Ti + Fe)]

$$r(\text{corr}) = C \cdot r(\text{obs}). \quad (2)$$

These corrected O to cation ratios are also given in Table 2.

Figure 1 shows that the O increase became more significant in more Ti-rich spinels, when $x \geq 0.7$. The spinels in this region have y for samples synthesized at the boundary with ilmenite in the range of 0.06–0.10, which corresponds to the gain of 1.5–2.5 mol% O relative to reference samples. In Fe-rich spinels, the O gain does not exceed the error of its determination. This correlates with the less pronounced variation of unit-cell parameters for those compositions.

Discussion

Figure 4 shows a_0 values for spinels from two-phase boundary associations (spinel + rhombohedral phase, spinel + wüstite, spinel + Fe) or produced at f_{O_2} near the boundaries. The samples synthesized and quenched under most reducing conditions have systematically higher a_0 values for a given Ti/(Fe + Ti). These spinels, which are presumed to be stoichiometric and associated with wüstite, lie along the upper curve, which almost coincides with the unit-cell parameter curve from Wechsler et al. (1984) for compositions with $x < 0.7$.

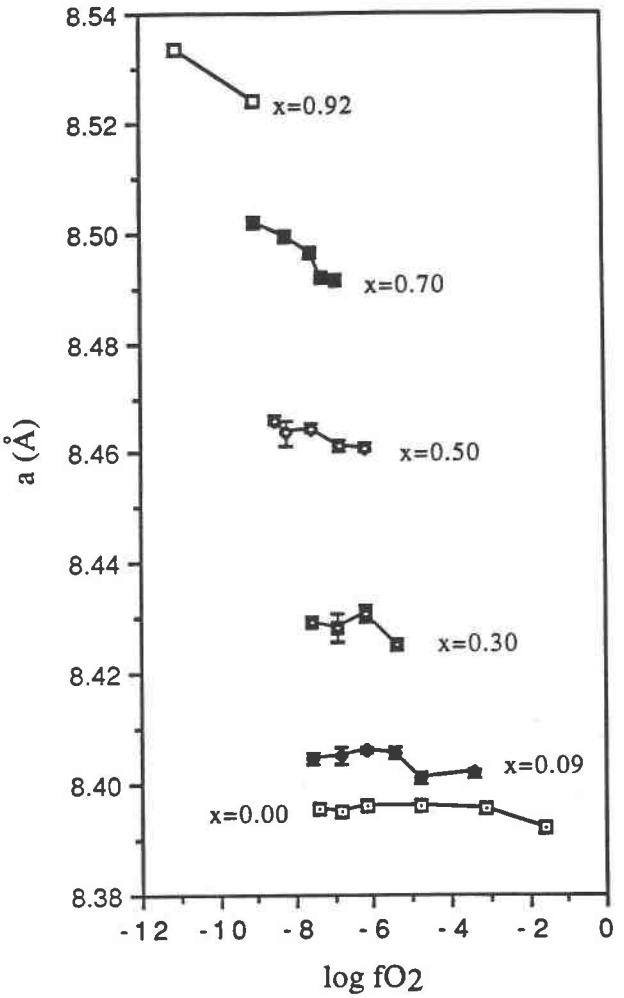

Fig. 3. Unit-cell parameter variation along O reaction lines for different spinel compositions.

For compositions with $x > 0.9$, the boundary ulvöspinel coexists with metallic Fe. The unit-cell parameter of this spinel does not vary strongly with composition.

The lower curve (Fig. 4) is for spinels coexisting with the rhombohedral phase. The decrease in a_0 of these samples is further evidence for nonstoichiometry. The direction of the unit-cell parameter change is the same as in the case of low-temperature spinel oxidation and the formation of Ti-bearing maghemite (Readman and O'Reilly, 1972; Nishitani and Kono, 1983).

The a_0 value of quenched spinels correlates with composition (Fig. 4), confirming the s-shaped dependence of a_0 on the Ti/(Ti + Fe) ratio in both the stoichiometric and nonstoichiometric series (Lindsley, 1965; Banerjee et al., 1967; Wechsler et al., 1984). However, their studies did not consider the nonstoichiometry, y. The dependence of the a_0 decrease on a change in y is shown in Figure 5. Data for spinel pairs of the same Ti/(Fe + Ti)

TABLE 2. Microprobe analyses and phase compositions

Sample	Fe (wt%)	Ti (wt%)	O (wt%)	TOTAL (wt%)	Fe (at%)	Ti (at%)	O (at%)
			x = 0–0.1				
78* (n** = 9)	72.599(182)	0.000	27.590(177)	100.189	42.982(107)	0.000	57.018(365)
87 (n = 5)	72.594(252)	0.008(7)	27.750(155)	100.352	42.836(149)	0.006(5)	57.158(319)
34 (n = 5)	70.366(161)	1.856(25)	27.600(62)	99.822	41.668(95)	1.281(17)	57.050(126)
62 (n = 6)	70.303(137)	1.880(8)	27.582(94)	99.765	41.655(81)	1.299(6)	57.046(194)
23 Sp (n = 7)	70.935(146)	1.363(48)	27.618(35)	99.916	41.991(86)	0.941(33)	57.068(72)
			x = 0.5				
74* (n = 6)	61.063(267)	10.465(114)	28.638(216)	100.166	35.250(154)	7.043(77)	57.707(435)
10 (n = 5)	61.452(269)	10.370(92)	28.996(117)	100.818	35.164(154)	6.918(61)	57.917(234)
			x = 0.7				
32* (n = 5)	57.456(116)	14.968(38)	27.276(63)	99.699	33.774(68)	10.258(26)	55.968(129)
28 (n = 5)	57.356(77)	14.996(44)	27.734(131)	100.086	33.415(45)	10.186(30)	56.400(266)
47 Sp (n = 5)	56.769(104)	15.396(44)	27.633(65)	99.798	33.164(61)	10.487(30)	56.349(133)
			x > 0.9				
51* (n = 19)	51.257(282)	19.837(163)	29.450(171)	100.544	28.929(159)	13.053(107)	58.018(337)
42 (n = 10)	50.055(157)	20.934(39)	29.678(175)	100.127	28.211(88)	13.401(26)	58.387(344)
43 (n = 14)	51.521(160)	19.294(100)	30.025(239)	100.840	28.811(89)	12.579(65)	58.609(467)
73 Sp (n = 5)	49.792(85)	20.150(19)	29.460(193)	99.402	28.272(48)	13.339(13)	58.389(383)
75 Sp (n = 3)	49.297(158)	20.597(42)	29.450(131)	99.344	27.992(90)	13.636(28)	58.372(260)
54 (n = 7)	48.717(116)	21.356(50)	29.734(326)	99.807	27.461(65)	14.035(32)	58.504(641)
72 (n = 7)	48.687(227)	21.607(162)	29.533(108)	99.827	27.512(128)	14.235(107)	58.253(213)
83 Sp (n = 5)	47.722(174)	22.538(97)	29.752(134)	100.012	26.832(98)	14.775(64)	58.393(263)

* Reference sample.
** Number of analyses.
† On the base of Ti + Fe = 3.

ratio are used to find Δa and Δy values. These pairs are samples 34-62, 78-87, 72-54, 71-10, 51-43, 32-38, and 42-73 (Table 2). A correlation between the Δy increase and the a_0 decrease appears to exist independent of Ti/(Fe + Ti), and a 0.01-Å decrease in a_0 corresponds, on average, to a Δy = 0.08 O gain. The unit-cell parameter, therefore, does serve as an indicator of nonstoichiometry. We suggest that part of the decrease in the data of Wechsler et al. (1984) for a_0 of magnetite-ulvöspinel solutions with $x > 0.7$ can be attributed to deviation from stoichiometry, which, though it was not characterized by Wechsler et al., was also not excluded.

Figure 6 shows proposed phase relations. The nonstoichiometry range of quenched spinels decreases as the magnetite content increases.

Transformation from a stoichiometric phase $Fe_{3-x}Ti_xO_4$ to a nonstoichiometric phase $Fe_{3-x}Ti_xO_{4+y}$, resulting from oxidation, can be described as

$$(1 + x)Fe^{2+} + [(1 + x)z/4]O_2 \rightarrow (1 + x)(1 - z)Fe^{2+} + [(1 + x)z]Fe^{3+} + [(1 + x)z/2]O^{2-} + [3(1 + x)z/8]\square. \quad (3)$$

Here z is the atomic fraction of oxidized Fe^{2+} ions in the total number $(1 + x)$ of Fe^{2+} in an unoxidized initial specimen. Then $y = \frac{1}{2}(1 + x)z$. This expression permits us to calculate z from O gain data, y, and estimate the Fe^{2+}/Fe^{3+} ratio in spinels (Table 2).

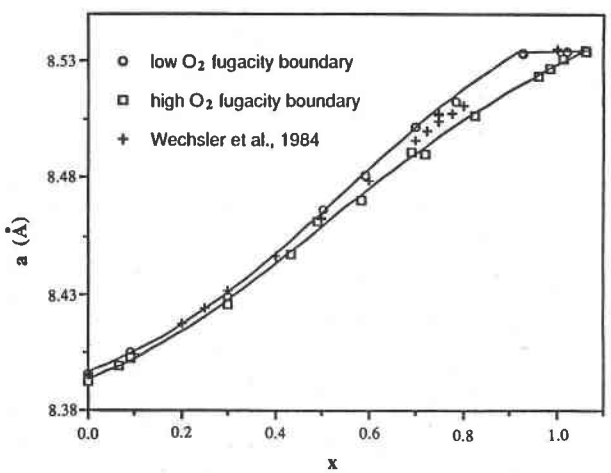

Fig. 4. Unit-cell parameter variation along high and low f_{O_2} boundaries of the spinel field.

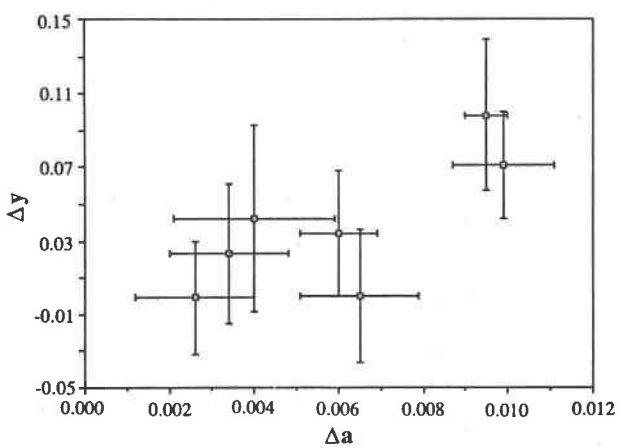

Fig. 5. Correlation of y with a_0 change.

TABLE 2—*Continued*

Sample	Ti/(Ti + Fe) (measured)	O/(Ti + Fe) (measured)	O/(Ti + Fe) (corrected)	Fe†	Ti†	O†	Fe^{2+}/Fe^{3+}
			$x = 0–0.1$				
78* ($n^{**} = 9$)	0.0000	1.3266(92)	1.3333(92)	3.000	0.000	4.000(28)	0.500
87 ($n = 5$)	0.0001	1.3442(89)	1.3410(127)	3.000	0.000	4.023(38)	0.466
34 ($n = 5$)	0.0298(4)	1.3284(45)	1.3351(101)	2.911(1)	0.089(1)	4.005(30)	0.597
62 ($n = 6$)	0.0302(1)	1.3280(45)	1.3346(102)	2.909(1)	0.091(1)	4.004(31)	0.593
23 Sp ($n = 7$)	0.0219(8)	1.3293(17)	1.3360(94)	2.934(3)	0.066(3)	4.008(28)	0.557
			$x = 0.5$				
74* ($n = 6$)	0.1665(16)	1.3645(103)	1.3333(100)	2.500(5)	0.500(5)	4.000(30)	0.498
10 ($n = 5$)	0.1644(13)	1.3763(56)	1.3448(114)	2.507(4)	0.493(4)	4.034(34)	1.318
			$x = 0.7$				
32* ($n = 5$)	0.2330(6)	1.2711(29)	1.3333(31)	2.301(2)	0.699(2)	4.000(9)	2.822
28 ($n = 5$)	0.2336(6)	1.2936(61)	1.3569(96)	2.999(2)	0.701(2)	4.071(29)	2.105
47 Sp ($n = 5$)	0.2402(6)	1.2908(30)	1.3541(45)	2.279(2)	0.721(2)	4.062(13)	2.338
			$x > 0.9$				
51* ($n = 19$)	0.3109(21)	1.3820(80)	1.3333(77)	2.067(6)	0.933(6)	4.000(23)	14.360
42 ($n = 10$)	0.3220(8)	1.4031(83)	1.3537(112)	2.034(3)	0.966(3)	4.061(34)	9.705
43 ($n = 14$)	0.3039(12)	1.4160(113)	1.3661(135)	2.088(4)	0.912(4)	4.098(41)	4.605
73 Sp ($n = 5$)	0.3206(4)	1.4031(92)	1.3537(119)	2.038(1)	0.962(1)	4.061(36)	9.273
75 Sp ($n = 3$)	0.3276(8)	1.4022(62)	1.3528(99)	2.017(3)	0.983(3)	4.058(30)	12.410
54 ($n = 7$)	0.3382(11)	1.4100(154)	1.3601(169)	1.985(3)	1.015(3)	4.081(51)	21.340
72 ($n = 7$)	0.3410(19)	1.3955(51)	1.3464(93)	1.977(6)	1.023(6)	4.039(28)	60.780
83 Sp ($n = 5$)	0.3551(13)	1.4035(63)	1.3541(99)	1.935(4)	1.065(4)	4.062(30)	—

Oxidation (Reaction 3) is accompanied by a vacancy formation. Vacancies can also result from an Fe-Ti substitution:

$$2Fe^{2+} \rightarrow \square + Ti^{4+}. \quad (4)$$

This mechanism must be the only one effective for the formation of nonstoichiometric spinel on the FeO-TiO_2 join (Fig. 6). This is probably the case for sample 83 (Table 2). It is a nonstoichiometric spinel formed, with ilmenite, near the low f_{O_2} limit of the spinel field. It is reasonable to assume that, for this very Ti-rich sample synthesized under strongly reducing conditions, Fe^{3+} is absent, and Ti^{3+} can probably be neglected. Although a small amount of Ti^{3+} was proposed as a component in the ulvöspinel solid solution in equilibrium with ilmenite and Fe at this temperature (Simons and Woermann, 1978), direct evidence of its existence is lacking, and in any case, the Ti^{3+} fraction in the spinel must be very small.

Figure 6 shows that coexisting spinel and ilmenite compositions (Table 1) are linked by connode lines. It follows that it is the ilmenite solid solution that would preferentially accommodate Ti^{3+} in equilibrium with ulvöspinel. Equilibrium joins between ulvöspinel and ilmenite have slopes pointing at the relative enrichment of a high Ti rhombohedral phase by reduced cations.

The composition of a nonstoichiometric spinel may be expressed as $(Fe_m Ti_n \square_q)_3 O_4$. From electron microprobe analysis (Tables 1, 2), $n/(m + n)$ is known. Together with electroneutrality ($2m + 4n = 8$) and cation site number ($m + n + q = 3$), we have enough constraints to find m, n, and q. The calculations for the spinel phase from sample 83 give $(Fe_{1.904}Ti_{1.048}\square_{0.048})O_4$ or $(Fe_{1.935}Ti_{1.065})O_{4.065}$. The estimated value of $y = 0.065$ is very close to the analytical data for this sample ($y = 0.062$, Table 2). This consistency supports both the above assumptions and the electron microprobe analysis for O.

The data on spinel oxidation obtained here for quenched samples contradict Taylor's (1964) suggestion that O gain does not depend on Ti/(Fe + Ti). The present data also are at variance with Dieckmann's (1982) estimations of O increase in oxidized magnetite up to 2 mol% at 1300 °C. We observe such O contents only in the high Ti part of the system. Dieckmann's values were obtained directly at high temperature, whereas ours are from quenched samples. It is reasonable to presume that this may account for the difference, and that quenching the fully oxidized state becomes more difficult with increasing Fe content because of the ease of electron transfer through Fe^{2+}-Fe^{3+} hopping mechanisms.

The ability to lose and gain O may be further related to the Fe^{2+}/Fe^{3+} ratio in the spinel and the cation distri-

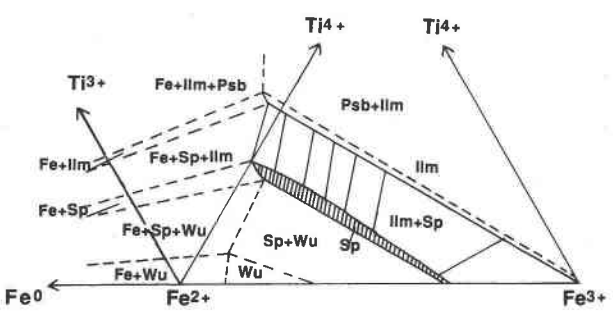

Fig. 6. Quenched spinel solid-solution region (shaded) and adjoining phase field in the Fe-Ti-O system. Abbreviations the same as on Fig. 1. Thin lines in the Ilm + Sp field link coexisting compositions.

Table 3. Comparison of O content determination by electron microprobe and Rutherford backscattering methods

Sample	Formula	Microprobe (y)	Rutherford back-scattering (y)	Complete oxidation calculated (y)
28	$Fe_{2.30}Ti_{0.70}O_{4+y}$	0.07(03)	0.57(10)	0.85
32	$Fe_{2.30}Ti_{0.70}O_{4+y}$	0.00(01)	0.00(09)	0.85
42	$Fe_{2.03}Ti_{0.97}O_{4+y}$	0.06(03)	0.13(09)	0.98
43	$Fe_{2.09}Ti_{0.91}O_{4+y}$	0.10(04)	0.29(10)	0.96
78	$Fe_{3.00}O_{4+y}$	0.00(03)	0.08(10)	0.50

bution. Fe^{3+} has an apparent energetic preference for tetrahedral sites (Blasse, 1964; Navrotsky and Kleppa, 1967; O'Neill and Navrotsky, 1983). Therefore, Fe^{2+} in these sites may be energetically somewhat easier to oxidize. Oxidized Fe tends to be tetrahedrally surrounded, even in excess of the number of normally occupied tetrahedral sites, and can occupy, after oxidation, some tetrahedral interstitial sites to preserve fourfold coordination for Fe^{3+} (Goss, 1988).

The Fe^{3+} preference for tetrahedral sites may be another reason for preferential loss of O by Fe-rich spinels during quenching. Above 1200 °C, differently charged cations in magnetite are almost randomly distributed over tetrahedral and octahedral sites (Wu and Mason, 1981; Schmalzried, 1983a, 1983b) (if indeed one can distinguish Fe^{2+} and Fe^{3+} at all). At low temperatures, magnetite is an inverse spinel. An oxidized spinel at low temperatures would have to contain excess Fe^{3+} and vacancies on octahedral sites. The rapid process of cation ordering upon quench may conceivably expel the excess $^{[6]}Fe^{3+}$ together with O loss.

Fe-rich and Ti-rich compositions differ also in the extent of the stability range along the f_{O_2} axis. The defect chemistry is not similar at low and high f_{O_2}, as shown in magnetite by a tracer diffusion study (Dieckmann, 1982). Although under more oxidizing conditions magnetite has a certain cation deficit and vacancies represent the defects, at low f_{O_2} some small cation excess can take place and Fe interstitials are predominant point defects. The position of the crossover from one regime to the other is approximately in the middle of the log f_{O_2} interval for magnetite. The concentration of interstitial Fe (δ in $Fe_{3+\delta}O_4$) equilibrated at 1300 °C at low f_{O_2} is $\sim 10^{-3}$. It is less by an order of magnitude than the cation deficit, $\delta \sim 10^{-2}$, caused by vacancy formation in the high O region. The concentration of interstitial defects is much less than the precision of our analytical method. From a chemical viewpoint, the concentration of interstitials can, therefore, be taken as virtually zero for samples in equilibrium with wüstite. This is just as we have assumed when choosing reference samples for electron microprobe analysis. We have further assumed that cation excess is insignificant across the entire composition range from Fe_3O_4 to Fe_2TiO_4, which appears reasonable in view of the above.

However, rigorous thermodynamic and structural consideration may require taking both types of defects into account (Aragon and McCallister, 1982). True stoichiometric compositions may lie at some distance in f_{O_2} from the boundary with wüstite, and for magnetite they are stable near the middle of the log f_{O_2} region (Dieckmann, 1982).

In more Ti-rich spinels, unit-cell parameters (Fig. 3) tend to decrease with increasing f_{O_2} in the whole interval of accessible f_{O_2}. This decrease is probably an indication of oxidation and vacancy formation in the whole f_{O_2} range. One might further hypothesize that the shrinking f_{O_2} extent of the spinel field with increasing Ti/(Ti + Fe) reflects a decrease in the (already very small) amount of interstitial Fe under reducing conditions.

An attempt was also made to analyze O content in the spinels by another technique. Daniele Cherniak from Rensselaer Polytechnic Institute investigated our samples by Rutherford backscattering (RBS) with H ions. The data (see Table 3) show a trend similar to that of the microprobe results. Samples that were identified as unoxidized in microprobe analyses have the lowest extent of oxidation in the Rutherford data (samples 78 and 32). However, oxidized nonstoichiometric spinels show by RBS significantly greater O contents, approaching values corresponding to complete oxidation of Fe^{2+} to Fe^{3+}. That probably means that the surface, which contributes significantly to RBS, may be much more oxidized than the bulk. That could occur during quench, or during subsequent sample handling in air.

Our analyzed samples are now ready for a high-temperature solution calorimetric study of mixing properties in the Fe_3O_4-Fe_2TiO_4–$Fe_{8/3}O_4$ system to detail the effects of both the Fe/Ti ratio and nonstoichiometry on thermodynamic properties. We defer discussion of thermodynamic consequences for activity-composition relations and oxide geothermometry-geobarometry till such studies are completed. Before destroying the samples by calorimetry, we are making Mössbauer measurements on them.

Conclusions

High and low f_{O_2} boundaries of the magnetite-ulvöspinel solution stability region are refined at 1300 °C, 1 atm.

The composition of magnetite-ulvöspinel solutions in equilibrium with wüstite at 1300 °C cannot exceed approximately 90 mol% Fe_2TiO_4. More Ti-rich spinels are formed at low f_{O_2} in equilibrium with metallic Fe and are nonstoichiometric.

Spinel solid solutions synthesized and quenched at higher f_{O_2} and equilibrated with the rhombohedral phase or produced near the boundary with it show an increase in O to cation ratio relative to samples synthesized at low f_{O_2}. O gain is greatest (2 mol%) in Ti-rich spinels ($x \geq 0.7$), corresponding to compositions $(Fe,Ti)_3O_{4.08}$. In high-Fe compositions ($x \geq 0.5$) the observed nonstoichiometry range in analyzed quenched species is two or more times less than in high-Ti samples.

The unit-cell parameter variation is a sensitive indi-

cator, not only of composition [Ti/(Ti + Fe)], but of high-temperature nonstoichiometric [O/(Ti + Fe)] ulvöspinel solid solutions.

Acknowledgments

We thank Jerry Delaney of Rutgers University for his help in microprobe analyses and Daniele Cherniak of Rensselaer Polytechnic Institute for Rutherford backscattering analyses. Also, we would like to acknowledge Charles Bennett, Nancy Brown, Douglas Johnson, and Krys Mocala for their help with laboratory procedures. This work was supported by the National Science Foundation grant DMR 89-12549.

References cited

Anderson, A.T. (1968) The oxygen fugacity of alkaline basalt and related magmas, Tristan da Cunha. American Journal of Science, 266, 707–727.

Appleman, D.E., and Evans, H.T., Jr. (1973) Indexing and least squares refinement of powder diffraction data. U.S. Geological Survey Computer Contribution, 20, 62 p.

Aragon, R., and McCallister, R.H. (1982) Phase and point defect equilibria in the titanomagnetite solid solution. Physics and Chemistry of Minerals, 8, 112–120.

Banerjee, S.K., O'Reilly, W., Gibb, T.C., and Greenwood, N.N. (1967) The behavior of ferrous ions in iron-titanium spinels. Journal of Physics and Chemistry of Solids, 28, 1323–1335.

Blasse, G. (1964) Crystal chemistry and some magnetic properties of mixed metal oxides with spinel structures. Phillips Research Reports Supplement, 3, 1–139.

Chou, I.-M. (1987) Oxygen buffer and hydrogen sensor techniques at elevated pressures and temperatures. In G.C. Ulmer and H.L. Barnes, Eds., Hydrothermal experimental techniques, p. 61–69. Wiley, New York.

Deines, P., Nafziger, R.H., Ulmer, G.C., and Woermann, E. (1974) Temperature-oxygen fugacity tables for selected gas mixtures in the system C-H-O at one atmosphere total pressure. Bulletin of the Earth and Mineral Sciences, Experiment Station, The Pennsylvania State University, 88, 129 p.

Dieckmann, R. (1982) Defects and cation diffusion in magnetite. IV. Nonstoichiometry and point defect structure of magnetite ($Fe_{3-\delta}O_4$). Berichte der Bunsen-Gesellschaft für physikalische Chemie, 86, 112–118.

Furuta, T., Otsuki, M., and Akimoto, T. (1985) Quantitative electron probe microanalysis of oxygen in titanomagnetites with implications for oxidation processes. Journal of Geophysical Research, 90, 3145–3150.

Goss, C.J. (1988) Saturation magnetisation, coercivity and lattice parameter changes in the system Fe_3O_4–γ Fe_2O_3, and their relationship to structure. Physics and Chemistry of Minerals, 16, 164–171.

Hauptman, Z. (1974) High temperature oxidation, range of non-stoichiometry and Curie point variation of cation deficient titanomagnetite $Fe_{2.4}Ti_{0.6}O_{4+\gamma}$. Geophysical Journal of the Royal Astronomical Society, 38, 29–47.

Katsura, T., Kitayama, K., Aoyagi, R., and Sasajima, S. (1976) High-temperature experiments related to Fe-Ti oxide minerals in volcanic rocks. Kazan (Volcanoes), 21, 31–56.

Lindsley, D.H. (1965) Iron-titanium oxides. Carnegie Institution of Washington Year Book, 64, 144–148.

Navrotsky, A., and Kleppa, O.J. (1967) The thermodynamics of cation distribution in simple spinels. Journal of Inorganic and Nuclear Chemistry, 29, 2701–2714.

Nishitani, T., and Kono, M. (1983) Curie temperature and lattice constant of oxidized titanomagnetite. Geophysical Journal of the Astronomical Society, 74, 585–600.

O'Neill, H.S.C., and Navrotsky, A. (1983) Simple spinels: Crystallographic parameters, cation radii, lattice energies and cation distributions. American Mineralogist, 68, 181–194.

Readman, P.W., and O'Reilly, W. (1972) Magnetic properties of oxidized (cation-deficient) titanomagnetites (Fe, Ti, $\square)_3O_4$. Journal of Geomagnetism and Geoelectricity, 24, 69–90.

Schmalzried, H. (1983a) Thermodynamics of compounds with narrow ranges of nonstoichiometry, Part I. Berichte der Bunsen-Gesellschaft für physikalische Chemie, 86, 112–118.

——— (1983b) Thermodynamics of compounds with narrow ranges of nonstoichiometry, Part II. Berichte der Bunsen-Gesellschaft für physikalische Chemie, 87, 726–733.

Simons, B., and Woermann, E. (1978) Iron titanium oxides in equilibrium with metallic iron. Contribution to Mineralogy and Petrology, 66, 81–89.

Taylor, R.W. (1964) Phase equilibria in the system FeO-Fe_2O_3-TiO_2 at 1300 °C. American Mineralogist, 49, 1016–1030.

Webster, A.H., and Bright, N.F.H. (1961) The system iron-titanium-oxygen at 1200 °C and oxygen partial pressure between 1 atm and 2×10^{-14} atm. Journal of the American Ceramic Society, 44, 110–116.

Wechsler, B.A., Lindsley, R., and Prewitt, C.T. (1984) Crystal structure and cation distribution in titanomagnetite ($Fe_{3-x}Ti_xO_4$). American Mineralogist, 69, 754–770.

Wu, C.C., and Mason, T.O. (1981) Thermopower measurement of cation distribution in magnetite. Journal of the American Ceramic Society, 64, 520–522.

Manuscript received May 5, 1992
Manuscript accepted January 20, 1993